

# Vortex lattices in a stirred Bose-Einstein condensate

K. W. Madison, F. Chevy, W. Wohlleben<sup>†</sup>, J. Dalibard  
 Laboratoire Kastler Brossel\*,  
 Département de Physique de l'Ecole Normale Supérieure  
 24 rue Lhomond, 75005 Paris, France

## Abstract

We stir with a focused laser beam a Bose-Einstein condensate of  $^{87}\text{Rb}$  atoms confined in a magnetic trap. We observe the formation of a single vortex for a stirring frequency exceeding a critical value. At larger rotation frequencies we produce states of the condensate for which up to eleven vortices are simultaneously present. We present measurements of the decay of a vortex array once the stirring laser beam is removed.

**Pacs:** 03.75.Fi, 67.40.Db, 32.80.Lg

## 1 Introduction

The discovery of Bose-Einstein condensation of atomic gases [1, 2, 3, 4] has led to a new impulse in the physics of quantum gases. Among the several questions that can be studied in these systems, superfluidity is one of the most intriguing and fascinating. A first hint to the superfluid behaviour of these systems was provided by the study of the oscillation frequencies of the normal modes of these systems [5]. A more direct evidence has been found by recent experiments aiming to study the energy deposited in the condensate by a moving “object” (*i.e.* the hole created by a blue detuned laser)[6] and the rotational properties of the gas [7, 8, 9].

The relation between the rotational and superfluid properties of a gas or a liquid is illustrated by the famous “rotating bucket” experiment (see Fig. 1). When an ordinary fluid is placed in a rotating container, the steady state corresponds to a rotation of the fluid as a whole together with the vessel. The velocity field for a normal fluid is the same for a rigid rotating body:

$$\mathbf{v} = \boldsymbol{\Omega} \times \mathbf{r} . \quad (1)$$

Superfluidity, first observed in liquid HeII, changes dramatically this behaviour [10, 11, 12, 13, 14]. Indeed, for a low enough rotation frequency, the superfluid is not entrained at all by the walls of the rotating bucket, and it stays at rest in the laboratory frame.

For a more quantitative description of the superfluid phenomenon, consider a Bose-Einstein condensate with weak, repulsive interactions (see *e.g.* [12, 13, 15]). This model is relevant for the  $^{87}\text{Rb}$  gas that we investigate experimentally since (i) the scattering length  $a$  characterizing the two-body interactions is positive, (ii) the “gaseous” parameter  $(\bar{\rho}a^3)^{1/2}$  is much smaller than 1 ( $\bar{\rho}$  is the average spatial density of the condensate). When cooled well below the condensation temperature, nearly all the atoms occupy the same state, and we can write the condensate wave

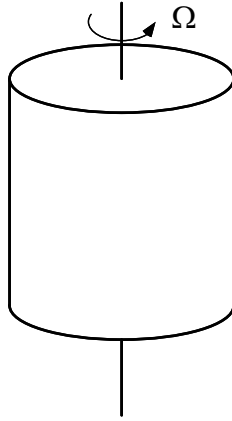


Figure 1: The rotating bucket experiment. A fluid is placed in a cylindrical container, which is rotated at a constant angular frequency  $\Omega$  along its axis. The velocity field at equilibrium reflects the superfluid character of the gas or the liquid. Indeed, for a low enough rotation frequency, the superfluid is not entrained at all by the walls of the rotating bucket, and it stays at rest in the laboratory frame.

function as  $\psi(\mathbf{r}) = \sqrt{\rho(\mathbf{r})} e^{iS(\mathbf{r})}$ , where  $\rho(\mathbf{r})$  is the spatial density. The velocity field is given by  $m\mathbf{v} = \hbar\nabla S$ , which is manifestly irrotational. This fact forbids, in particular, the rigid-body velocity field given in (1). An energy analysis, which is outlined in the next section of this paper for the particular case of harmonic confinement, leads to the following conclusions. For a low enough angular rotation frequency  $\Omega$ , the ground state is the same as that when the bucket is at rest. In this state, the phase of the condensate is constant over the whole volume and no rotational motion occurs. However above a critical frequency  $\Omega_c$ , a line of singularity, *i.e.* a vortex line, appears. The condensate density drops to zero on axis, and the phase of the condensate wave function is now given by  $S(\mathbf{r}) = \theta$ , where  $\theta$  is the azimuthal angle around the vortex axis (oriented along  $z$ ). The corresponding velocity field varies as  $r^{-1}$ , where  $r$  is the distance to the vortex center. Moreover, the velocity field has a quantized circulation around the axis:

$$\oint \mathbf{v} \cdot d\mathbf{r} = \frac{2\pi\hbar}{m}, \quad (2)$$

where  $m$  is the mass of the particles in the fluid. For frequencies notably higher than  $\Omega_c$ , one might expect that a single vortex line with a quantum number  $n$  larger than 1 would appear ( $S(\mathbf{r}) = n\theta$ ). However this state is unstable [12, 13, 14] and fragments into  $n$  vortices each with a unit circulation quantum.

These phenomenon have been observed in experiments with superfluid liquid helium; however, the model of a dilute Bose gas presented in the previous paragraph is not applicable to this dense system. Let us quote here two milestones in this very rich field of research. In 1958 Vinen performed an experiment in which he detected the presence of a single vortex filament by observing the induced frequency shift of the vibrational modes of a wire at the center of a rotating liquid helium bath [16]. In 1982 Yarmchuk and Packard obtained images of a vortex lattices in the superfluid by imaging electrons initially trapped at the cores of the vortex lines [17].

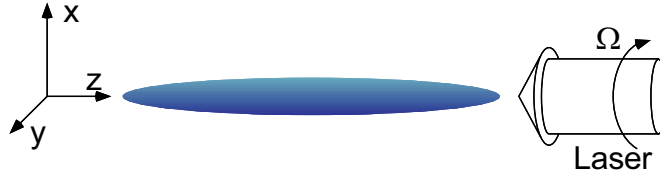


Figure 2: A cigar-shaped atomic cloud confined in an axisymmetric magnetic trap is stirred by a far-detuned laser beam. The laser beam propagates along the long axis of the cigar ( $z$ ), and it creates a dipole potential which is anisotropic in the  $xy$  plane. This anisotropy rotates around the  $z$  axis at the angular frequency  $\Omega$ .

## 2 Vortices in trapped gaseous condensates

The generation of quantized vortices in trapped atomic gases has been the subject of numerous theoretical studies in the recent years. Two schemes have been considered. The first one uses laser beams to engineer the phase of the condensate wave function and produce the desired velocity field [18, 19, 20, 21, 22]. Recently this scheme [21] has been successfully applied to a binary mixture of condensates, resulting in a quantized rotation of one of the two components around the second one [7]. Phase imprinting has also been used for the generation of solitons inside a condensate [23, 24].

The second scheme, which is explored in the present work, is directly analogous to the rotating bucket experiment [25, 26]. The atoms are confined in a static, cylindrically-symmetric Ioffe-Pritchard magnetic trap upon which we superimpose a non-axisymmetric, attractive dipole potential created by a stirring laser beam (see figure 2). The combined potential leads to a cigar-shaped harmonic trap with a slightly anisotropic transverse profile. The transverse anisotropy is rotated at angular frequency  $\Omega$  as the gas is evaporatively cooled to Bose-Einstein condensation, and it plays the role of the bucket wall roughness.

In this scheme, the formation of vortices is a consequence of thermal equilibrium. In the frame rotating at the same frequency as the anisotropy, the Hamiltonian is time-independent and one can use a standard thermodynamics approach to determine the steady-state of the system. In this frame, the Hamiltonian can be written  $\tilde{H} = H - \Omega L_z$ , where  $H$  is the Hamiltonian in the absence of rotation, and  $L_z$  is the total orbital angular momentum along the rotation axis. For a gas with repulsive interactions, the term  $-\Omega L_z$  may favor the creation of a state where the condensate wave function has an angular momentum  $\hbar$  along the  $z$  axis and therefore contains a vortex filament [27, 28, 29, 30, 31, 32, 33, 34, 35, 36].

This is illustrated in figure 3, which displays the lowest eigenenergies for the Gross-Pitaevski equation describing a gas with  $N$  atoms confined in a two-dimensional isotropic harmonic potential of frequency  $\omega_t$ :

$$-\frac{\hbar^2}{2m}\Delta\psi + \frac{1}{2}m\omega_t^2(x^2 + y^2)\psi + \frac{4\pi\hbar^2 Na}{m}|\psi|^2\psi = E\psi. \quad (3)$$

Here  $a$  is the scattering length characterizing the 2-body interaction. In figure 3a, we consider an ideal gas ( $a = 0$ ). The ground state found for  $\Omega = 0$ , which has zero angular momentum, remains the ground state of the system until the stirring frequency  $\Omega$  reaches  $\omega_t$ . Above this value, the gas is no longer stable since the centrifugal force  $m\Omega^2\mathbf{r}$  exceeds the restoring force of the confining potential  $-m\omega_t^2\mathbf{r}$ . For a gas with repulsive interactions (figure 3b), the energy of the state with angular momentum  $\ell = 1$  crosses the energy of the  $\ell = 0$  state at a critical value

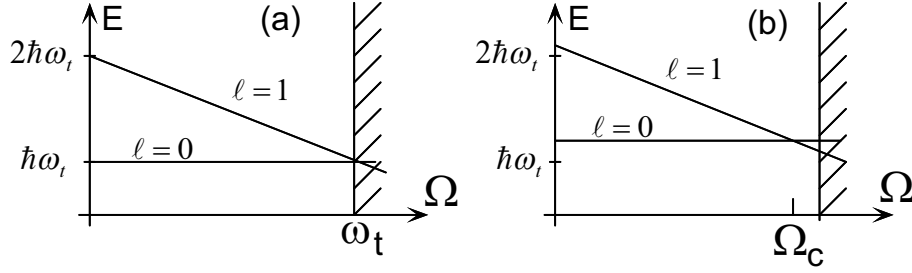


Figure 3: Lowest transverse energy levels for the Gross-Pitaevski equation of a gas confined in a bi-dimensional harmonic potential with frequency  $\omega_t$ , and stirred at an angular frequency  $\Omega$ . (a) In absence of interaction the ground state of the system is the same as that for  $\Omega = 0$  for any stirring frequency in the stability domain  $\Omega < \omega_t$ . (b) For an interacting gas with repulsive interactions (assumed here to be weak), there exists a critical frequency  $\Omega_c$  above which the ground state of the system has an angular momentum  $\ell = 1$ . The effect of the stirring anisotropy on the energy levels has been neglected.

$\Omega_c < \omega_\perp$ . Indeed one can infer that for  $\Omega = \omega_\perp$  the energy of the state  $\ell = 1$  is strictly below the energy of the state  $\ell = 0$ : (i) these two states have the same energy in absence of interactions for  $\Omega = \omega_t$ ; (ii) repulsive interactions increase the energy of these states, by an amount which is larger for the  $\ell = 0$  state, since it has a smaller volume than the state with  $\ell = 1$ .

When the interactions are large enough to reach the Thomas-Fermi limit, for which the kinetic energy is negligibly small compared to the potential and interaction energies, the solution of (3) for  $\ell = 1$  leads to a radius for the vortex core of the order of the healing length  $\xi = (8\pi a\rho)^{-1/2}$ , where  $\rho$  is the density of the condensate at the center of the trap in the absence of a vortex [5].

### 3 Experimental setup and determination of $\Omega_c$

Our set-up has been described in detail previously [37, 8], and we only briefly outline the main elements. The atoms are confined in an Ioffe-Pritchard magnetic trap. The slow oscillation frequency of the elongated magnetic trap is  $\omega_z/(2\pi) = 11.7$  Hz ( $z$  is horizontal in our setup), while the transverse oscillation frequency is  $\omega_\perp/(2\pi) = 219$  Hz. Bose-Einstein condensation is reached using evaporative cooling produced by a chirped radio-frequency source. For the data presented here, the final frequency of the evaporation ramp is chosen only a few kHz above the value which completely empties the trap. This guarantees that the temperature of the atomic gas is below 80 nK, the uncondensed cloud being only marginally visible. The number of atoms in the condensate is of the order of 140 000.

The stirring laser beam is switched on approximately at the time when the cloud reaches the condensation point. It propagates along the slow axis of the magnetic trap. The beam waist is  $w_s = 20.0 (\pm 1) \mu\text{m}$  and the laser power  $P$  is 0.4 mW. The recoil heating induced by this far-detuned beam (wavelength 852 nm) is negligible. Two crossed acousto-optic modulators, combined with a proper imaging system, allow for an arbitrary translation of the laser beam axis with respect to the symmetry axis of the condensate.

The motion of the stirring beam consists in the superposition of a fast and a slow component. The optical spoon's axis is toggled at a high frequency (100 kHz) between two symmetric

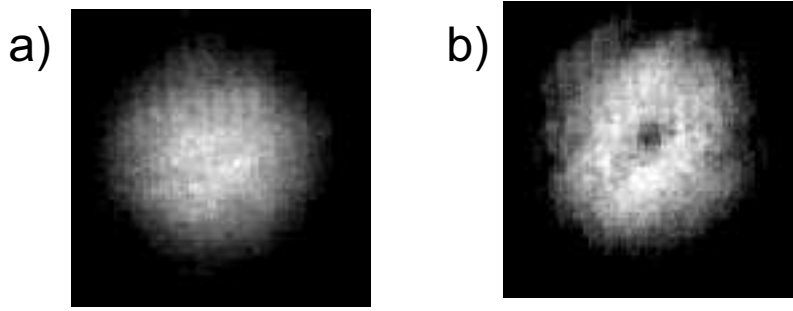


Figure 4: Absorption images of a Bose-Einstein condensate stirred with a laser beam (after a 27 ms time-of-flight). For both images, the condensate number is  $N_0 = (1.4 \pm 0.5) 10^5$  and the temperature is below 80 nK. The rotation frequency  $\Omega/(2\pi)$  is respectively (a) 145 Hz; (b) 152 Hz.

positions about the long trap axis  $z$ . The intersections of the stirring beam axis and the  $z = 0$  plane are  $\pm a(\cos \theta \mathbf{u}_x + \sin \theta \mathbf{u}_y)$ , where the distance  $a$  is  $8 \mu\text{m}$ . The fast toggle frequency is chosen to be much larger than the magnetic trap frequencies so that the atoms experience an effective two-beam, time-averaged potential. The slow component of the motion is a uniform rotation of the angle  $\theta = \Omega t$ . The value of the angular frequency  $\Omega$  is maintained fixed during the evaporation at a value chosen between 0 and  $2\pi \times 220 \text{ rad s}^{-1}$ .

The dipole potential, proportional to the power of the stirring beam, is well approximated by  $m\omega_{\perp}^2(\epsilon_X X^2 + \epsilon_Y Y^2)/2$ . The  $(X, Y)$  basis is rotated with respect to the fixed axes  $(x, y)$  by the angle  $\theta(t)$ , and  $\epsilon_X = 0.03$  and  $\epsilon_Y = 0.09$  for the parameters given above [38]. The action of this beam is essentially a slight modification of the transverse frequencies of the magnetic trap while the longitudinal frequency is nearly unchanged. The overall stability of the stirring beam on the condensate appears to be a crucial element for the success of the experiment, and we estimate that our stirring beam axis is fixed to and stable on the condensate axis to within  $2 \mu\text{m}$ .

After the end of the evaporation ramp, we let the system reach thermal equilibrium in this “rotating bucket” for a duration  $t_r = 500 \text{ ms}$ . The vortices induced in the condensate by the optical spoon are then studied using a time-of-flight analysis (27 ms) after the atoms have been released from the magnetic trap. Due to the atomic mean field energy, the initial cigar shape of the atomic cloud transforms into a pancake shape during the free fall. The transverse  $xy$  and longitudinal  $z$  sizes grow by a factor of 40 and 1.2 respectively [39]. In addition, the core size of the vortex should expand at least as fast as the transverse size of the condensate [39, 40, 41]. Therefore a vortex with an initial diameter  $2\xi = 0.4 \mu\text{m}$  for our experimental parameters is expected to grow to a size of  $16 \mu\text{m}$ .

At the end of the time-of-flight period, we illuminate the atomic sample with a resonant probe laser for  $20 \mu\text{s}$ . The shadow of the atomic cloud in the probe beam is imaged onto a CCD camera with an optical resolution  $\sim 7 \mu\text{m}$ . The probe laser propagates along the  $z$ -axis so that the image reveals the column density of the cloud after expansion along the stirring axis.

For the trap parameters given above, we have found that no singularity appears in the cloud image as long as the stirring frequency is smaller than 149 Hz. However, for a stirring frequency equal to or above 150 Hz (but smaller than 160 Hz, see next section) a density dip systematically appears at the center of the cloud. Figure 4 illustrates this transition by showing two pictures of the condensate after expansion; the first with a stirring frequency  $\Omega = 145 \text{ Hz}$  (Fig.4a) below

and the second  $\Omega = 152$  Hz (Fig.4b) above the critical frequency.

The dip in the optical density can reach up to 50% of the maximal column density and it constitutes an unambiguous signature of the presence of a vortex filament. In particular it cannot be induced by a mechanical action of the stirring laser, which in fact creates a restoring force towards the center of the magnetic trap since it is detuned red of resonance. The fact that the density does not vanish in the dip may be due to several reasons: (i) The vortex filament may not be perfectly straight but rather an oscillating line (the so-called Thomson mode [13]). (ii) Some non-condensed atoms may be trapped in the core of the vortex. (iii) The core diameter after expansion of  $\sim 18 \mu\text{m}$  at the half max of the dip is not much larger than the resolution limit of the imaging optics.

Finally, we note that the critical frequency is notably larger than the predicted value of 91 Hz [30] (see also [27, 29, 34, 32]). This deviation may be due to the marginality of the Thomas-Fermi approximation for our relatively low condensate number.

## 4 Dynamics of a vortex array

When the stirring frequency is increased notably above the value  $\Omega_c$ , multiple dips appear in the absorption image of the cloud. Each of these dips has approximately the same spatial width as the single dip of Fig. 4. For the trap parameters given above, the threshold frequency for the appearance for such multi-vortex patterns is 160 Hz, and condensates with up to 4 vortices have been observed [8].

We have found that we can generate patterns with more than 4 vortices if we reduce the transverse trapping frequency. This can easily be done by adjusting the value of the bias magnetic field at the center of the trap. The data that we give now have been obtained with a transverse frequency of  $\omega_t / 2\pi = 169$  Hz and a longitudinal frequency of  $\omega_z / 2\pi = 11.7$  Hz, the same as before.

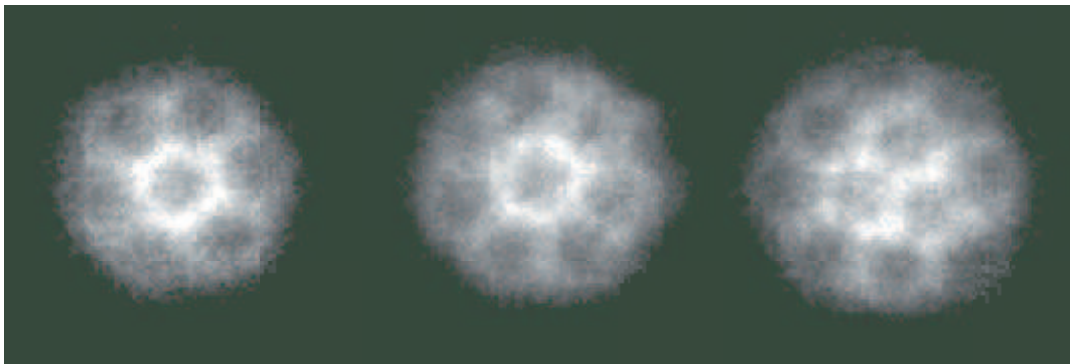


Figure 5: Arrays of vortices in a Bose-Einstein condensate stirred by a laser beam (after a 27 ms time-of-flight). These pictures have been obtained with a magnetic trap less stiff than for the pictures of Fig.4 ( $\omega_t / 2\pi = 169$  Hz).

For an atom number similar to the previous data ( $\sim 150\,000$ ), the critical frequency is now  $\Omega_c / 2\pi = 119$  Hz. This still corresponds to a ratio  $\Omega_c / \omega_t \sim 0.7$ . When we increase the stirring frequency above 130 Hz, arrays of several vortices can be observed. For instance, Fig.5 shows images of condensates with 7, 8 and 11 vortices. These three images have all been obtained with the same experimental conditions ( $\Omega / 2\pi = 135$  Hz), apart from residual shot-to-shot

fluctuations. In the pictures with 7 and 8 vortices (Fig.5a and Fig.5b), one vortex is found at the center of the trap, and the remaining ones form a regular hexagon or heptagon. The 11-vortex pattern (Fig.5c) has 3 vortices forming an equilateral triangle surrounded by a regular octagon. Some of the dips of the octagon are hardly visible, since they are located at the border of the condensate cloud.

In [8] we studied the lifetime of the one vortex pattern of Fig.4b when the stirring laser is removed. We found that this structure may survive for up to  $\sim 1$  s before decaying, proving the metastability of the current associated with the vortex [42]. We now present similar data obtained for a multiple vortex structure. For this experiment we chose a rotation frequency of  $\Omega = 135$  Hz and adjusted the number of atoms in the condensation to maximize the probability that a 5-vortex pattern form. For each point in the decay study, a vortex lattice is formed, then the stirring beam is turned off, and the condensate is allowed to evolve in the pure magnetic trap for an adjustable time. A time-of-flight analysis is performed to determine the number of vortices still present.

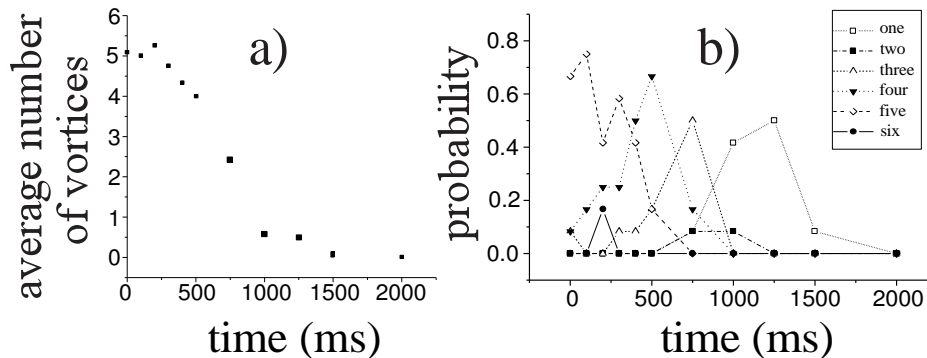


Figure 6: Decay of a vortex array. (a) Average number of vortices as a function of time spent by the gas in the axisymmetric trap after the end of the stirring phase. (b) Fraction of the images displaying  $n$  vortices as a function of time. After 2 seconds all pictures exhibit a condensate with no vortex.

The results are displayed in Fig.6 which presents the decay of the average number of vortices as a function of time, each point representing the average of 10 shots. The characteristic time for the reduction by a factor 2 of this average number is 750 ms. A more detailed representation is shown in Fig.6b which displays the fraction of pictures showing  $n$  vortices ( $n = 0, \dots, 6$ ) as a function of time. It seems apparent that the vortex pattern decays by losing one vortex at a time. For instance, at time  $t = 100$  ms, 9 patterns out of 10 exhibit 5 vortices; 400 ms later, 7 patterns out of 10 exhibit 4 vortices. It is remarkable that the vortex pattern readjusts itself shortly after the loss of a vortex. For instance, the 3-vortex patterns are found most often as a quasi-centered and quasi-equilateral triangle, while the 4-vortex patterns have essentially a square shape.

## 5 Conclusion

We have reported the formation of single and multiple-vortex structures in a gaseous Bose-Einstein condensate when it is stirred by a laser beam which produces a slight rotating anisotropy. We have also presented measurements of the lifetime of the pattern of vortices

when the rotating anisotropy is removed.

Several extensions of this work can be considered. Direct evidence for the quantized circulation of the velocity field (Eq.2) could be obtained either from an interferometric measurement similar to the one performed in [6] (see *e.g.* [34] or [22]), or from a study of the elementary excitations of the vortex filament [43, 44, 45]. Also the role of the thermal component in the nucleation and decay of the vortex pattern remains to be elucidated [32, 34, 46, 47, 48]. The rotational properties of the gas before the condensation point, where the collisional dynamics can be described by the classical or quantum Boltzmann equation, constitute other very interesting questions [49]. Finally, the scattering of quasi-resonant light by this medium may lead to spectacular phenomena, such as a “black hole” type behaviour when the speed of sound or mass flow in the condensate exceeds that of light [50].

We wish to dedicate this paper to the memory of Dan Walls who has had a seminal influence on the field of quantum optics in general, and in the understanding of the physics of gaseous Bose Einstein condensates in particular.

**Acknowledgments:** we thank V. Bretin, Y. Castin, C. Cohen-Tannoudji, C. Deroulers, D. Guéry-Odelin, C. Salomon, G. Shlyapnikov, S. Stringari, and the ENS Laser cooling group for several helpful discussions and comments. This work was partially supported by CNRS, Collège de France, DRET, DRED and EC (TMR network ERB FMRX-CT96-0002). This material is based upon work supported by the North Atlantic Treaty Organization under an NSF-NATO grant awarded to K.M. in 1999.

<sup>†</sup> permanent address: Max Planck Institute für KernPhysik, Heidelberg, Germany.

\* Unité de Recherche de l'Ecole normale supérieure et de l'Université Pierre et Marie Curie, associée au CNRS.

## References

- [1] M. H. Anderson, J. Ensher, M. Matthews, C. Wieman, and E. Cornell, *Science* **269**, 198 (1995).
- [2] C. C. Bradley, C. A. Sackett, and R. G. Hulet, *Phys. Rev. Lett.* **78**, 985 (1997); see also C. C. Bradley, C. A. Sackett, J. J. Tollett, and R. G. Hulet, *Phys. Rev. Lett.* **75**, 1687 (1995).
- [3] K. B. Davis, M.O. Mewes, N. Van Druten, D. Durfee, D. Kurn, and W. Ketterle, *Phys. Rev. Lett.* **75**, 3969 (1995).
- [4] D. Fried, T. Killian, L. Willmann, D. Landhuis, S. Moss, D. Kleppner, and T. Greytak, *Phys. Rev. Lett.* **81**, 3811 (1998).
- [5] For a review, see *e.g.* A. S. Parkins and D. Walls, *Phys. Rep.* **303**, 1 (1998); F. Dalfovo, S. Giorgini, L. P. Pitaevskii, and S. Stringari, *Rev. Mod. Phys.* **71**, 463 (1999).
- [6] C. Raman, M. Khl, R. Onofrio, D. S. Durfee, C. E. Kuklewicz, Z. Hadzibabic, and W. Ketterle, *Phys. Rev. Lett.* **83**, 2502 (1999).
- [7] M. R. Matthews, B. P. Anderson, P. C. Haljan, D. S. Hall, C. E. Wieman, and E. A. Cornell, *Phys. Rev. Lett.* **83**, 2498 (1999).



- [8] K. Madison, F. Chevy, W. Wohlleben, and J. Dalibard, Phys. Rev. Lett. **84**, 806 (2000).
- [9] O. M. Maragò, S. A. Hopkins, J. Arlt, E. Hodby, G. Hechenblaikner, and C. J. Foot, Phys. Rev. Lett. **84**, 2056 (2000).
- [10] L. Onsager, Nuovo Cimento **6**, suppl. 2, 249 (1949).
- [11] R.P. Feynman, in “Progress in Low Temperature Physics”, vol. 1, ed. by C.J. Gorter (North-Holland, Amsterdam, 1955) Chapter 2.
- [12] P. Nozières and D. Pines, *The Theory of Quantum Liquids*, vol. II (Addison Wesley, Redwood City, 1990).
- [13] E.M. Lifshitz and L. P. Pitaevskii, *Statistical Physics, Part 2*, chap. III (Butterworth-Heinemann, Oxford, 1980).
- [14] R.J. Donnelly, *Quantized Vortices in Helium II*, (Cambridge, 1991).
- [15] K. Huang, *Statistical Mechanics*, John Wiley (New-York, 1963).
- [16] W.F. Vinen, Nature **181**, 1524 (1958) and Proc. Roy. Soc. A **260**, 218 (1961).
- [17] E. J. Yarmchuck and R. E. Packard, J. Low Temp. Phys. **46**, 479 (1982).
- [18] K.P. Marzlin and W. Zhang, Phys. Rev. Lett. **79**, 4728 (1997).
- [19] R. Dum, J. I. Cirac, M. Lewenstein, and P. Zoller, Phys. Rev. Lett. **80**, 2972 (1998).
- [20] K.G. Petrosyan and L. You, Phys. Rev. A **59**, 639 (1999).
- [21] J. Williams and M. Holland, Nature **401**, 568 (1999).
- [22] L. Dobrek, M. Gajda, M. Lewenstein, K. Sengstock, G. Birkel, and W. Ertmer, Phys. Rev. A **60**, R3381 (1999).
- [23] S. Burger, K. Bongs, S. Dettmer, W. Ertmer, K. Sengstock, A. Sanpera, G. V. Shlyapnikov, and M. Lewenstein, Phys. Rev. Lett. **83**, 5198 (1999).
- [24] J. Denschlag, J.E. Simsarian, D.L. Feder, C. Clark, L.A. Collins, J. Cubizolles, L. Deng, E.W. Hagley, K. Helmerson, W.P. Reinhardt, S.L. Rolston, B.I. Schneider, and W.D. Phillips, Science **287**, 97 (2000).
- [25] A.J. Leggett, Topics in Superfluidity and superconductivity, in *Low Temperature Physics*, Edts M. Hoch and R. Lemmer (Springer-Verlag, 1992).
- [26] S. Stringari, Phys. Rev. Lett. **82**, 4371 (1999).
- [27] G. Baym and C.J. Pethick, Phys. Rev. Lett. **76**, 6 (1996).
- [28] F. Dalfavo and S. Stringari, Phys. Rev. A **53**, 2477 (1996).
- [29] S. Sinha, Phys. Rev. A **55**, 4325 (1997).
- [30] E. Lundh, C. J. Pethick, and H. Smith, Phys. Rev. A **55**, 2126 (1997).
- [31] D. Butts and D. Rokhsar, Nature **397**, 327 (1999).
- [32] D. L. Feder, C. W. Clark, and B. I. Schneider, Phys. Rev. Lett. **82**, 4956 (1999).

- [33] A. Fetter, J. Low. Temp. Phys. **113**, 189 (1998).
- [34] Y. Castin and R. Dum, Eur. Phys. J. D. **7**, 399 (1999).
- [35] B. M. Caradoc-Davies, R. J. Ballagh and K. Burnett, Phys. Rev. Lett. **83**, 895 (1999).
- [36] H. Pu, C. K. Law, J. H. Eberly and N. P. Bigelow, Phys. Rev. A **59**, 1533 (1999).
- [37] J. Söding, D. Guéry-Odelin, P. Desbiolles, F. Chevy, H. Inamori, J. Dalibard, Appl. Phys. B **69**, 257 (1999).
- [38] We observed that the vortex formation is not sensitive to the exact value of  $\epsilon_X, \epsilon_Y$ , and a single vortex state under the same conditions was successfully created with a laser power of half and twice the value of 0.4 mW used here.
- [39] Y. Castin and R. Dum, Phys. Rev. Lett. **77**, 5315 (1996).
- [40] E. Lundh, C. J. Pethick, and H. Smith, Phys. Rev. A **58**, 4816 (1998).
- [41] F. Dalfovo and M. Modugno, cond-mat/9907102.
- [42] D. Rokhsar, Phys. Rev. Lett. **79**, 2164 (1997).
- [43] R. Dodd, K. Burnett, M. Edwards, C. W. Clark, Phys. Rev. A **56**, 587 (1997).
- [44] F. Zambelli and S. Stringari, Phys. Rev. Lett. **81**, 1754 (1999).
- [45] A. Svidzinsky and A. Fetter, Phys. Rev. A. **58**, 3168 (1998).
- [46] T. Isoshima and K. Machida, Phys. Rev. A **60**, 3313 (1999).
- [47] A. Svidzinsky and A. Fetter, cond-mat/9811348.
- [48] P. Fedichev and G. Shlyapnikov, Phys. Rev. A **60**, R1779 (1999).
- [49] D. Guery-Odelin, cond-mat/0003024
- [50] U. Leonhardt and P. Piwnicki, Phys. Rev. Lett. **84**, 822 (2000).